PERGAMON

International Journal of Solids and Structures 36 (1999) 3517–3539

INTERNATIONAL JOURNAL OF SOLIDS and STRUCTURES

Natural frequencies of composite plates with tailored thermal residual-stresses

Sérgio Frascino Müller de Almeida[a,1], Jorn S. Hansen[b,*]

[a] *Instituto Tecnológico de Aeronaútica, Department of Mechanical Engineering, 12.228-900 São José dos Campos-SP, Brazil*

[b] *University of Toronto, Institute for Aerospace Studies, 4925 Dufferin Street, Downsview, Ontario, Canada M3H 5T6*

Received 22 November 1997; in revised form 1 May 1998

Abstract

Thermal residual-stresses introduced during manufacture and their effect on the natural frequencies and vibration modes of stringer stiffened composite plates is investigated. The principal idea in the work is to include stiffeners on the perimeter of a composite plate in which the laminate design of the stiffeners and plate are different. Such an arrangement yields manufacturing induced thermal residual-stresses; these stresses result from the difference in manufacturing and operating temperatures as well as the difference in thermal expansion coefficients and elastic properties of the plate and the stiffeners. The analysis is based on an enhanced Reissner–Mindlin plate theory and involves two separate calculations. In the first, the thermal residual-stress state is determined for an unconstrained plate. In the second, the free vibration problem is solved; thermal effects from the first calculation are included by way of nonlinear membrane-bending coupling which in turn defines the free vibration reference state. The problem is solved using a 16-node bi-cubic Lagrange element in a finite element formulation. Three different plate-stiffener geometries are used to illustrate the effects of stringer size, stringer placement and temperature difference. Two principal results are obtained: first, it is shown that thermal residual-stresses can have a significant effect on the natural frequencies; secondly, thermal residual-stresses can be tailored to increase natural frequencies. Therefore it is concluded that an evaluation of these stresses and a judicious analysis of their effects must be included in the design of this class of composite structures.

Nomenclature

b	reinforcement width
$[B]$	matrix relating linear strain components and nodal displacements
$[B_G]$	matrix relating non-linear strain components and nodal displacements

* Corresponding author. Fax: 001 416 667 7799; E-mail: hansen@bach.utias.utoronto.ca

[1] Currently on leave at UTIAS.

PII: S0020–7683(98)00154–1

$[\mathscr{D}]$ constitutive matrix between middle-surface linear strains and resultant forces
$[\mathscr{D}_{\mathscr{G}}]$ constitutive matrix between middle-surface non-linear strains and resultant forces
$\{e\}$ vector of linear strain components
$\{e_G\}$ vector of non-linear strain components
$\{\bar{f}\}$ vector of edge tractions
I moment of inertia
$[\mathscr{I}]$ inertia matrix
$[K]$ global stiffness matrix
$[K]_p$ stiffness matrix for p-th element
$[K_G^R]$ global geometric stiffness matrix
$[K_G^R]_p$ geometric stiffness matrix for p-th element
L Lagrangian
m mass per unit area
$\{M\}_t$ vector of resultant moments
$[M]$ global mass matrix
$[M]_p$ mass matrix for p-th element
n number of elements in finite element model
$\{N\}_t$ vector of resultant forces
$[N]$ matrix of interpolation functions
$[Q]$ matrix of material stiffnesses
T kinetic energy
$\bar{u}$ displacement in x-direction
u middle-surface displacement in x-direction
$\{\bar{u}\}$ vector of displacements
U strain energy
$\bar{v}$ displacement in x-direction
v middle-surface displacement in y-direction
$\bar{w}$ displacement in x-direction
w middle-surface displacement in z-direction
W work of external forces
z_k z-coordinate of the top of the k-th layer
$\{\bar{\alpha}\}$ vector of thermal expansion coefficients
$\{\delta\}$ global vector of nodal displacements
$\{\delta_p\}$ vector of nodal displacements for p-th element
ΔT change in temperature
$\{\bar{\varepsilon}\}$ vector of strain components
$\{\bar{\varepsilon}^L\}$ vector of linear strain components
$\{\bar{\varepsilon}^N\}$ vector of non-linear strain components
$\{\kappa\}$ vector of middle-surface curvatures
Φ total potential energy
ψ_x middle-surface rotation variable in x-direction
ψ_y middle-surface rotation variable in y-direction
ρ mass density
$\{\bar{\sigma}_R\}$ vector of thermal residual stresses

1. Introduction

It is well established that initial and/or residual stresses affect the flexural stiffness and in turn the dynamic and stability characteristics of isotropic plates, Herrmann and Armenakas (1960), Brunelle and Robertson (1974). Similar results are also true for laminated plates as demonstrated by Yang and Shieh (1987) and recently by Almeida and Hansen (1996).

The residual stresses in a plate may result from external applied loads, from environmental effects such as temperature or moisture absorption or a combination of environmental effects and boundary constraints. Such stresses may also arise during the manufacture of a plate because of elevated processing temperatures. Whitney and Ashton (1971) and, more recently, Sai Ram and Sinha (1992) analyzed environmental effects on the vibration characteristics of composite plates. These investigations dealt with stresses which develop because of boundary constraints when a laminated composite plate is subjected to temperature changes and moisture absorption. These problems have direct practical application for situations in which the structure providing the boundary constraint to the plate is not affect by such environmental changes.

On the other hand, very significant thermal residual-stresses may be introduced in composite structures during the manufacturing process and nominally similar structures may have significantly different residual-stress states. For example, thermal residual stresses in stringer reinforced plates/shells are very different if the structure is manufactured using co-cured methods in contrast to secondary bonding techniques. Such residual stresses and their implications are seldom included in structural design and analysis. In a recent paper, Almeida and Hansen (1996) have demonstrated very conclusively that the presence of such manufacturing stresses may substantially affect the elastic buckling response of stiffened composite plates. That result leads to the present work.

The thermal residual-stresses considered here arise during manufacture and are a consequence of the anisotropy of advanced composite materials. The thermal expansion coefficient of unidirectional graphite/epoxy composites is, for example, typically close to zero in the direction of the fibers and relatively large in the transverse direction. Therefore, thermal residual-stresses develop in a plate as it is cooled from the processing (cure, consolidation or bonding) temperature to room or operating temperature. It is important to emphasize that even in the presence of thermal residual-stresses, the in-plane thermal residual stress-resultants of classical plate theory are zero if there are no external constraints and if the composite design is invariant over the domain of the plate. Therefore, for this class of problem and within the context of linear-elastic, classical plate theory the residual stresses do not lead to any changes in elastic response. On the other hand, these stress resultants are in general non-zero if the composite design varies over the plate domain; for example if the laminate is non-homogeneous (a function of x, y) in the plane or contains non-uniformities such as stringers.

The objective of this work is to investigate the effect of manufacturing-introduced thermal residual-stresses on the free vibration response of stringer-reinforced composite plates; it is assumed that the thermoelastic design of the stringer and plate are different. Furthermore, it is assumed that the string-plate combination is co-cured and therefore the mismatch between the coefficient of thermal expansion of the stringer and plate results in thermal residual-stresses. The magnitude of these stresses depends on a number of factors such as plate and stringer geometry and design, physical properties of the composite materials, processing temperature and operating temperature.

The idea is to design a plate in which the thermal residual-stresses improve structural characteristics. In the present case, the thermal residual-stress state will be used to increase the natural frequencies of simply supported plates.

The scope of this work is restricted to the analysis of problems with no membrane–bending coupling; the out-of-plane deformations resulting from the elevated temperature processing of laminates with membrane–bending coupling leads to totally different analysis requirements. Laminates with membrane–bending coupling in general exhibit out-of-plane deflections at a temperature below the processing temperature. This means that at the operating temperature, the plate vibrates about a deformed, non-flat configuration. In such a situation, the vibration analysis must be taken with respect to a curved reference state. Based on curved panel analysis, to do otherwise would beg to introduce significant errors. The effect of thermal residual curvatures are not accounted for in the present analysis and the behaviour of non-symmetric laminates is therefore beyond the scope of the present work. This limitation should not be regarded as a major restriction as it does not affect conclusions of this work.

The analysis of the problem is based on a finite element formulation using a 16-node bi-cubic Lagrange element. Reissner–Mindlin plate theory is used to solve the thermal and the free vibration problem for three different stiffened-plate geometries. The calculations indicate that natural frequencies can be significantly increased by properly tailoring the residual stresses.

2. Problem formulation

The solution of the problem involves two steps. In the first, thermal residual-stresses are determined; in the second, the free vibration problem is solving including the stiffening due to the thermal residual-stresses obtained in the first step. All calculations are based on laminated Reissner–Mindlin plate theory.

A linear analysis is used to determine the distribution of thermal residual-stresses resulting from processing. For this calculation, the plate-stiffener assembly is assumed to be completely unconstrained; thus residual stresses arise only from the thermal coefficient of expansion mismatches either through the thickness of the laminate or due to spatial variations in the thermal coefficient of expansion.

A full nonlinear formulation is used to determine the reference state for the free vibration analysis. Thus the stress stiffening due to the thermal residual-stresses is included in the subsequent free vibration analysis. The free vibration problem is solved as a linear eigenvalue problem which yields natural frequencies and associated vibration modes.

2.1. Kinematic relations

A symmetrically-laminated, stringer-reinforced composite plate is considered. Each lamina is assumed to be orthotropic, homogeneous, linear elastic and is oriented at an angle θ measured counter-clockwise with respect to the x-axis.

The Mindlin plate model is adopted Mindlin (1951). Therefore, the in-plane displacement fields $\bar{u}$, $\bar{v}$ are assumed to vary linearly through the plate thickness and the transverse displacement $\bar{w}$ is assumed constant through the plate thickness. Throughout this work, an overline indicates a

quantity at an arbitrary point (x, y, z) in the plate and quantities without the overline are defined on the x–y plane at the plate middle-surface. Using this notation the assumed displacement field is written as:

$$\begin{aligned}\bar{u}(x,y,z) &= u(x,y) + z\psi_x(x,y)\\ \bar{v}(x,y,z) &= v(x,y) + z\psi_y(x,y)\\ \bar{w}(x,y,z) &= w(x,y)\end{aligned} \tag{1}$$

where u, v and w are the middle-surface displacements in the x-, y- and z-directions, respectively, while ψ_x and ψ_y are rotation like variables in the x-, y-directions, respectively.

The strain vector is represented as the sum of linear and non-linear components:

$$\{\bar{\varepsilon}\} = \{\bar{\varepsilon}^{\mathrm{L}}\} + \{\bar{\varepsilon}^{\mathrm{N}}\} \tag{2}$$

Based on the non-linear strain–displacement relations, Novozhilov (1953), the linear strain components are given by:

$$\begin{aligned}\bar{\varepsilon}_x^{\mathrm{L}} &= u_{,x} + z\kappa_{xx}\\ \bar{\varepsilon}_y^{\mathrm{L}} &= v_{,y} + z\kappa_{yy}\\ \bar{\gamma}_{xy}^{\mathrm{L}} &= u_{,y} + v_{,x} + z\kappa_{xy}\\ \bar{\gamma}_{xz}^{\mathrm{L}} &= w_{,x} + \psi_x\\ \bar{\gamma}_{yz}^{\mathrm{L}} &= w_{,y} + \psi_y\end{aligned} \tag{3}$$

where κ_{ij} are the middle-surface curvatures of the plate defined as

$$\begin{aligned}\kappa_{xx} &= \psi_{x,x}\\ \kappa_{yy} &= \psi_{y,y}\\ \kappa_{xy} &= \psi_{x,y} + \psi_{y,x}\end{aligned} \tag{4}$$

Also, $\{\varepsilon\}$ is used to represent the vector of in-plane linear strain components:

$$\{\varepsilon\}^T = [u_{,x} \quad v_{,y} \quad u_{,y} + v_{,x}] \tag{5}$$

The non-linear strain components, expressed in terms of the displacements, are:

$$\begin{aligned}\bar{\varepsilon}_x^{\mathrm{N}} &= \tfrac{1}{2}[(u_{,x}^2 + v_{,x}^2 + w_{,x}^2) + 2z(u_{,x}\psi_{x,x} + v_{,x}\psi_{y,x}) + z^2(\psi_{x,x}^2 + \psi_{y,x}^2)]\\ \bar{\varepsilon}_y^{\mathrm{N}} &= \tfrac{1}{2}[(u_{,y}^2 + v_{,y}^2 + w_{,y}^2) + 2z(u_{,y}\psi_{x,y} + v_{,y}\psi_{y,y}) + z^2(\psi_{x,y}^2 + \psi_{y,y}^2)]\\ \bar{\gamma}_{xy}^{\mathrm{N}} &= (u_{,x}u_{,y} + v_{,x}v_{,y} + w_{,x}w_{,y}) + z(u_{,x}\psi_{x,y} + u_{,y}\psi_{x,x} + v_{,x}\psi_{y,y} + v_{,y}\psi_{y,x}) + z^2(\psi_{x,x}\psi_{x,y} + \psi_{y,x}\psi_{y,y})\\ \bar{\gamma}_{xz}^{\mathrm{N}} &= (u_{,x}\psi_x + v_{,x}\psi_y) + z(\psi_x\psi_{x,x} + \psi_y\psi_{y,x})\\ \bar{\gamma}_{yz}^{\mathrm{N}} &= (u_{,y}\psi_x + v_{,y}\psi_y) + z(\psi_x\psi_{x,y} + \psi_y\psi_{y,y})\end{aligned} \tag{6}$$

In the above and in the following, a subscript following a comma indicates partial differentiation with respect to that variable.

Strain at any point in the plate can be described in terms of the middle-surface strains using eqns (3)–(6). Therefore, a middle-surface linear strain vector, $\{e\}$, and a vector of the components of the non-linear strain terms, $\{e_G\}$ are defined as:

$$\{e\}^T = [u_{,x} \quad v_{,y} \quad u_{,y}+v_{,x} \quad \kappa_{xx} \quad \kappa_{yy} \quad \kappa_{xy} \quad w_{,x}+\psi_x \quad w_{,y}+\psi_y] \tag{7}$$

$$\{e_G\}^T = [u_{,x} \quad u_{,y} \quad v_{,x} \quad v_{,y} \quad w_{,x} \quad w_{,y} \quad \psi_{x,x} \quad \psi_{x,y} \quad \psi_{y,x} \quad \psi_{y,y} \quad \psi_x \quad \psi_y] \tag{8}$$

2.2. Thermal problem

The first step in the analysis is the computation of the thermal residual-stresses in the plate. When calculating the thermal residual-stresses, it is assumed that: the plate is totally unconstrained, there are no mechanical loads, there is no membrane–bending coupling in the laminate and the analysis is linear. (No nonlinear geometric effects.)

Since it is assumed that strain–displacement relation is linear, the stress–strain relations including thermal effects become

$$\{\bar{\sigma}\} = [\bar{Q}]\{\{\bar{\varepsilon}^L\} - \Delta T\{\bar{\alpha}\}\} \tag{9}$$

where $[\bar{Q}]$ are the material stiffnesses in structural coordinates; $\{\bar{\varepsilon}^L\}$ is the vector of total strains; $\{\bar{\alpha}\}$ is the vector of lamina thermal coefficients of expansion (expressed in structural coordinates) and ΔT is the change in temperature. The expressions for $[\bar{Q}]$ and $\{\bar{\alpha}\}$ in terms of lamina elastic properties are given by Jones (1975).

It is to be noted that the material properties are in general functions of temperature and at elevated temperatures viscoelastic/creep effects are to be expected. These effects are not considered here but may be important in practical applications. However, results are presented for a range of ΔT and these illustrate that the effects being investigated are insignificant for a broad range of ΔT. The viscoelastic/creep effects can be accounted for approximately if the value of ΔT is regarded as the difference between the room temperature and an 'equivalent processing temperature'.

Thermal residual stresses are determined by seeking a stationary value of the total potential energy when the system is subject only to a thermal change. That is:

$$\Phi^t = \frac{1}{2}\int_A \{e\}^T[\mathscr{D}]\{e\}\,\mathrm{d}A - \Delta T\int_A (\{\varepsilon\}\{N\}_t + \{\kappa\}\{M\}_t)\,\mathrm{d}A \tag{10}$$

where the superscript on Φ^t indicates thermal. In the above, A is the area of the plate, $[\mathscr{D}]$ is the constitutive matrix relating the stress resultants and the middle-surface strains, while $\{N\}_t$ and $\{M\}_t$ are thermal load vectors.

Matrix $[\mathscr{D}]$ is defined by:

$$[\mathscr{D}] = \begin{bmatrix} [A] & [B] & [0] \\ [B] & [D] & [0] \\ [0] & [0] & [A^*] \end{bmatrix} \tag{11}$$

where

$$(A_{ij}, B_{ij}, D_{ij}) = \sum_{k=1}^{K} \int_{z_{k-1}}^{z_k} [\bar{Q}_{ij}]_k (1, z, z^2)\, \mathrm{d}z \quad i,j = 1,2,6 \tag{12}$$

and

$$A^*_{ij} = \sum_{k=1}^{K} \int_{z_{k-1}}^{z_k} [\bar{Q}_{ij}]_k\, \mathrm{d}z \quad i,j = 4,5 \tag{13}$$

where K is the total number of lamina and z_{k-1}, z_k are the coordinates of the bottom and top of the k-th layer with respect to the plate middle-surface.

The thermal load vectors are defined as, Jones (1975):

$$\{N\}_t = \Delta T \sum_{k=1}^{K} [\bar{Q}]_k \{\bar{\alpha}\}_k (z_k - z_{k-1}) \tag{14}$$

and

$$\{M\}_t = \Delta T \sum_{k=1}^{K} [\bar{Q}]_k \{\bar{\alpha}\}_k \frac{(z_k^2 - z_{k-1}^2)}{2} \tag{15}$$

It must be noted that, even though this work is restricted to laminates with no membrane–bending coupling, the above formulation includes the membrane–bending coupling matrix, $[B]$, and thermal moments, $\{M\}_t$. These entities were introduced in the formulation for completeness. The bending thermal residual-stress resultants $\{M\}_t$ and matrix $[B]$ are identically zero for all the problems analysed in this work.

The finite element calculation solves the thermal displacement field corresponding to a stationary value of eqn (10); then, the thermal residual-stresses in the plate are obtained by back substituting into eqn (9).

2.3. Free vibration problem

The second step in the problem is the free vibration analysis. This calculation is considered as a linear perturbation about a nonlinear reference state which results from the previous thermal calculation; in this way the effects of the initial thermal residual-stresses are incorporated in the vibration problem.

The equations of motion for the plate can be derived from Hamilton's principle. The Lagrangian, L, is given by:

$$L = T - \Phi \tag{16}$$

where T is the kinetic energy and Φ is the potential energy of the plate. In turn $\Phi = U - W$ where U is the strain energy and W is the work of the applied forces.

In the free vibration problem, the stresses at any point in the plate are given by:

$$\{\bar{\sigma}\} = [\bar{Q}]\{\bar{\varepsilon}\} + \{\bar{\sigma}_R\} = [\bar{Q}]\{\bar{\varepsilon} + \bar{\varepsilon}_R\} \tag{17}$$

where $\{\bar{\sigma}_R\}$, $\{\bar{\varepsilon}_R\}$ are the thermal residual stresses and strains, respectively, while $\{\bar{\varepsilon}\}$ is the total

strain resulting from the vibrational motion. Matrix $[\bar{Q}]$ is the constitutive relation in xyz reference axes for the particular lamina under consideration.

The potential energy of the plate can be computed from:

$$\Phi = U - W = \frac{1}{2}\int_v \{\bar{\varepsilon}+\bar{\varepsilon}_R\}^T\{\bar{\sigma}\}\,\mathrm{d}v - \int_s \{\bar{f}\}^T\{\bar{u}\}\,\mathrm{d}s \tag{18}$$

where v is the entire volume of the plate and s is its surface; $\{\bar{u}\}$ are the displacements, and $\{\bar{f}\}$ are the edge tractions.

No edge tractions are present in the free vibration problem and therefore, $W \equiv 0$ and $\Phi = U$. Substituting eqn (2) and (17) into eqn (18), neglecting higher-order terms and using the fact that $\{\bar{\sigma}_R\}$ correspond to a state of equilibrium, yields the result:

$$U = \frac{1}{2}\int_v \{\bar{\varepsilon}^{\mathrm{L}}\}^T[\bar{Q}]\{\bar{\varepsilon}^{\mathrm{L}}\}\,\mathrm{d}v + \int_v \{\bar{\varepsilon}^{\mathrm{N}}\}^T\{\bar{\sigma}_R\}\,\mathrm{d}v \tag{19}$$

The strain energy is now integrated through the thickness (with respect to z) after using eqns (3), (4) and (6). The resulting expression can be written in terms of the middle-surface strain vector, $\{e\}$ and the components of the non-linear strain terms, $\{e_G\}$ defined, respectively, in eqns (7) and (8). Equation (19) becomes:

$$U = \frac{1}{2}\int_A \{e\}^T[\mathscr{D}]\{e\}\,\mathrm{d}A + \frac{1}{2}\int_A \{e_G\}^T[\mathscr{D}_G^R]\{e_G\}\,\mathrm{d}A \tag{20}$$

where matrix $[\mathscr{D}]$ represents the constitutive relation between the stress resultants and the middle-surface strains as given in eqn (11).

The terms in eqn (20) involving the subscript G refer to the strain energy due to the coupling between linear and non-linear terms. The linear terms refer to the thermal residual stresses indicated by superscript R. It can be shown that matrix $[D_G^R]$ is given by:

$$[\mathscr{D}_G^R] = \begin{bmatrix}
N_x^R & N_{xy}^R & 0 & 0 & 0 & 0 & M_x^R & M_{xy}^R & 0 & 0 & Q_x^R & 0 \\
N_{xy}^R & N_y^R & 0 & 0 & 0 & 0 & M_{xy}^R & M_y^R & 0 & 0 & Q_x^R & 0 \\
0 & 0 & N_x^R & N_{xy}^R & 0 & 0 & 0 & 0 & M_x^R & M_{xy}^R & 0 & Q_y^R \\
0 & 0 & N_{xy}^R & N_y^R & 0 & 0 & 0 & 0 & M_{xy}^R & M_y^R & 0 & Q_y^R \\
0 & 0 & 0 & 0 & N_x^R & N_{xy}^R & 0 & 0 & 0 & 0 & 0 & 0 \\
0 & 0 & 0 & 0 & N_{xy}^R & N_y^R & 0 & 0 & 0 & 0 & 0 & 0 \\
M_x^R & M_{xy}^R & 0 & 0 & 0 & 0 & L_x^R & L_{xy}^R & 0 & 0 & T_x^R & 0 \\
M_{xy}^R & M_y^R & 0 & 0 & 0 & 0 & L_{xy}^R & L_y^R & 0 & 0 & T_y^R & 0 \\
0 & 0 & M_x^R & M_{xy}^R & 0 & 0 & 0 & 0 & L_x^R & L_{xy}^R & 0 & T_x^R \\
0 & 0 & M_{xy}^R & M_y^R & 0 & 0 & 0 & 0 & L_{xy}^R & L_y^R & 0 & T_y^R \\
Q_x^R & Q_x^R & 0 & 0 & 0 & 0 & T_x^R & T_y^R & 0 & 0 & 0 & 0 \\
0 & 0 & Q_y^R & Q_y^R & 0 & 0 & 0 & 0 & T_x^R & T_y^R & 0 & 0
\end{bmatrix} \tag{21}$$

The following stress resultants were used in the definition of matrix $[\mathscr{D}_G^R]$:

$$(N_{ij}^R, M_{ij}^R, L_{ij}^R) = \sum_{k=1}^{K} \int_{z_{k-1}}^{z_k} \bar{\sigma}_{ij}^R(1, z, z^2)\,\mathrm{d}z \quad ij = xx, yy, xy \tag{22}$$

and

$$(Q_i^R, T_i^R) = \sum_{k=1}^{K} \int_{z_{k-1}}^{z_k} \bar{\sigma}_{iz}^R(1, z)\,\mathrm{d}z \quad i = x, y \tag{23}$$

It should be noted that L_{ij}^R are higher-order moments of the stress about the plate middle-surface; these stress resultants are in general non-zero. Also, the kinematic hypotheses imply that the stress resultants T_i^S are identically zero for symmetrically laminated plates; they may be non-zero for non-symmetric laminates. These latter terms are included in the formulation only for the sake of completeness.

The kinetic energy of the plate is:

$$T = \frac{1}{2}\int_v \left\{\begin{matrix}\dot{\bar{u}}\\ \dot{\bar{v}}\\ \dot{\bar{w}}\end{matrix}\right\}^T \left\{\begin{matrix}\dot{\bar{u}}\\ \dot{\bar{v}}\\ \dot{\bar{w}}\end{matrix}\right\} \rho\,\mathrm{d}v \tag{24}$$

where ρ is the mass density. Since the mass distribution is uniform over the plate cross-section, the kinetic energy can be written in terms of the middle-surface displacements as:

$$T = \frac{1}{2}\int_A \left\{\begin{matrix}\dot{u}\\ \dot{v}\\ \dot{w}\\ \dot{\psi}_x\\ \dot{\psi}_y\end{matrix}\right\}^T \begin{bmatrix} m & 0 & 0 & 0 & 0\\ 0 & m & 0 & 0 & 0\\ 0 & 0 & m & 0 & 0\\ 0 & 0 & 0 & I & 0\\ 0 & 0 & 0 & 0 & I \end{bmatrix} \left\{\begin{matrix}\dot{u}\\ \dot{v}\\ \dot{w}\\ \dot{\psi}_x\\ \dot{\psi}_y\end{matrix}\right\} \mathrm{d}A \tag{25}$$

where

$$(m, I) = \int_{z_0}^{z_K} (1, z^2)\rho\,\mathrm{d}z \tag{26}$$

3. Finite element formulation

The problem formulated in the previous section was solved using a finite element method. A 16-node isoparametric bi-cubic element using Lagrange interpolation functions was developed and

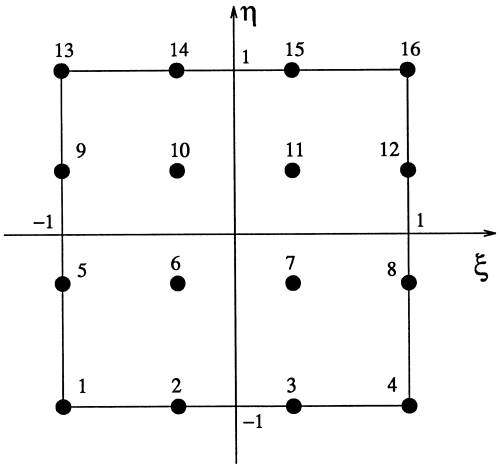

Fig. 1. Bi-cubic Lagrange isoparametric element.

implemented in a FORTRAN code. Figure 1 shows the geometry of the element. The nodal variables are the displacements and rotations: u, v, w, ψ_x, and ψ_y. Therefore, each element has a total of 80 degrees-of-freedom. The displacements at an arbitrary point within the domain of the p-th element are given by:

$$\{\delta\}^T = [u \quad v \quad w \quad \psi_x \quad \psi_y] = [N]\{\delta\}_p \tag{27}$$

where $[N]$ is a matrix of interpolation functions. Matrix $[N]$ has dimensions 5×80. Vector $\{\delta\}_p$ contains the 80 element nodal variables arranged as:

$$\{\delta\}_p^T = [u_1 \quad v_1 \quad w_1 \quad \psi_{x1} \quad \psi_{y1} \quad u_2 \quad \ldots \quad \psi_{y15} \quad u_{16} \quad v_{16} \quad w_{16} \quad \psi_{x16} \quad \psi_{y16}] \tag{28}$$

The vector of strains at the middle-surface of the plate can be expressed as:

$$\{e\} = [B]\{\delta\}_p \tag{29}$$

where matrix $[B]$ is a 8×80 matrix that contains derivatives of the interpolation functions N_i with respect to variables x and y. Matrix $[B]$ can be derived from eqn (3), (4), (27), and (29). The derivatives of the interpolation functions with respect to coordinates x and y were computed in terms of derivatives of the interpolation functions with respect to the element coordinates ξ and η, shown in Fig. 1. A general quadrilateral cubic isoparametric element was implemented. This allows the representation of complex geometries with a small number of elements. Similarly, the vector of components of the non-linear strain terms, $\{e_G\}$, can be computed as:

$$\{e_G\} = [B_G]\{\delta\}_p \tag{30}$$

where matrix $[B_G]$ is a 12×80 matrix that contains derivatives of the interpolation functions N_i with respect to variables x and y. Matrix $[B_G]$ can be derived from eqns (8), (27), and (30). Again, matrix $[B_G]$ was computed for a general quadrilateral element.

The element stiffness and geometric stiffness matrices are computed from the matrices defined above. The stiffness matrix of the p-th element is given by:

$$[K]_p = \int_A [B]^T[\mathscr{D}][B]\,\mathrm{d}A \tag{31}$$

The area integration of the p-th element is carried out numerically using 4×4 Gauss quadrature. A shear correction factor of 5/6 is used for all laminates. It should also be noted that the present element formulation does not suffer from shear locking and no special techniques or reduced integration are required, Heppler and Hansen (1986).

Similarly, the element geometric stiffness matrix incorporating the thermal residual-stresses for the p-th element is given by:

$$[K_G^R]_p = \int_{A_p} [B_G]^T[\mathscr{D}_G^R][B_G]\,\mathrm{d}A \tag{32}$$

The geometric stiffness matrices $[K_G^R]_p$ are calculated assuming a thermal stress state corresponding to the difference between the room temperature and the processing temperature. These matrices are also determined using 4×4 Gauss quadrature. As noted earlier, as a first step the thermal problem is solved and from these results the stress is determined at each Gauss point; this is the information required to compute the matrix $[\mathscr{D}_G^R]$.

The expression for the plate strain energy can now be rewritten using an approximation based on the finite element discretization. Equation (20) therefore, becomes:

$$U_n = \frac{1}{2}\sum_{p=1}^{n} \{\delta\}_p^T[K]_p\{\delta\}_p + \frac{1}{2}\sum_{p=1}^{n} \{\delta\}_p^T[K_G^R]_p\{\delta\}_p \tag{33}$$

where n is the total number of elements in the model.

The element mass matrix is derived from eqns (25) and (27) and yields the result:

$$[M]_p = \int_{A_p} [N]^T[\mathscr{I}][\mathscr{N}]\mathscr{A} \tag{34}$$

where the inertia matrix $[\mathscr{I}]$ is:

$$[\mathscr{I}] = \begin{bmatrix} m & 0 & 0 & 0 & 0 \\ 0 & m & 0 & 0 & 0 \\ 0 & 0 & m & 0 & 0 \\ 0 & 0 & 0 & I & 0 \\ 0 & 0 & 0 & 0 & I \end{bmatrix} \tag{35}$$

Using these definitions, the kinetic energy becomes:

$$T_n = \frac{1}{2}\sum_{p=1}^{n} \{\dot{\delta}\}_p^T[M]_p\{\dot{\delta}\}_p \tag{36}$$

Global matrices consistent with the boundary conditions of the problem are generated using conventional finite element techniques. Applying Hamilton's principle yields the equations of motion for the plate; assuming that the problem is unforced and that the solution is periodic yields

the free vibration problem. This equation is an eigenvalue problem in terms of the vector of unknown nodal displacements, $\{\delta\}$:

$$\{[K]+[K_G^R]-\omega^2[M]\}\{\delta\} = \{0\} \tag{37}$$

where $[M]$, $[K]$, and $[K_G^R]$ are the global matrices for the plate. The natural frequencies and corresponding vibration modes are the solution of the this problem; here it is solved using the subspace iteration algorithm, Bathe and Wilson (1976).

4. Vibration of plates with tailored thermal residual stresses

The numerical procedure implemented is suitable for the evaluation of the free vibration response of symmetric composite laminates in the presence of thermal residual-stresses. As noted earlier, behaviour of non-symmetric laminates is beyond the scope of the present work.

4.1. Types of reinforced plates analyzed

A square graphite/epoxy plate with stringer reinforcement is considered for illustrative purposes. The plate and stringer designs lead to non-homogeneous stiffness and thermal coefficients over the problem domain which introduces non-zero thermal residual stress resultants.

The basic laminate for the analysis is a $[0/90]_s$. Since only symmetric plates are considered, the reinforcement is always placed symmetrically along the edges of the plate and is of uniform width b. The concept is to use reinforcement made of unidirectional laminates because they have high stiffness and nearly zero thermal expansion coefficient; the plate itself will be designed with lower stiffness but with a larger thermal coefficient of expansion. It is assumed the structure is stress free at the processing temperature and that residual stresses develop during the cooling phase to room temperature. During the cooling process, the reinforcement contracts less than the plate and resists the tendency of the plate to shrink. This effect causes tensile residual-stresses in the plate and compressive residual stresses in the reinforcement. The distribution of the residual stresses depends on the material properties, lay-up sequence of plate and reinforcement as well as the geometric arrangement of the reinforcement. The resulting distribution of residual stresses may be either beneficial or detrimental to the mechanical behaviour of the plate depending on the particular problem under consideration.

Three different types of reinforced plates are considered. The reinforcement used for plates types I and II consists of four unidirectional plies of width b placed on both sides of a $[0/90]_s$ laminate. In plate type I the reinforcement is placed on the outer edges of the plate parallel to the y-axis with the fibers parallel to the y axis. In plate type II the reinforcement is placed around the perimeter of the plate forming a symmetric frame around the plate and the fibres are oriented parallel to the appropriate side of the plate. Figure 2 illustrates the geometry and lamination sequence for each of the configurations considered.

The configurations chosen for plates types I and II were designed to allow an assessment of the influence of the distribution of thermal residual stress resultants. In plate type I the thermal residual stress resultants are particularly high near the edges of the reinforcement. They tend to be zero at the center of the plate due to Saint Venant effects and large stress gradients are present. On the

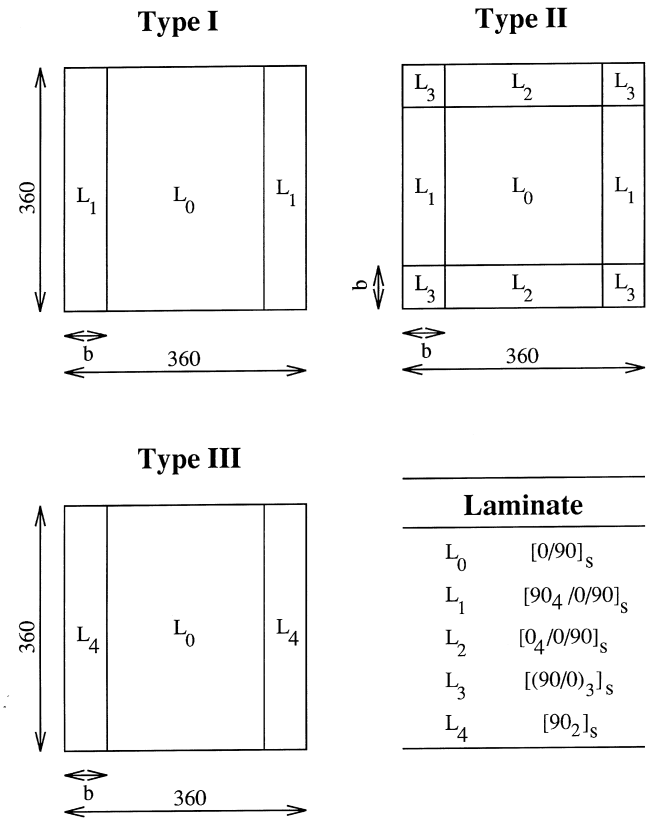

Fig. 2. Types of reinforced plates analyzed.

other hand, plate type II is stretched everywhere in both directions due to the frame constraint. The stress distribution is more uniform without large gradients.

The plate types analyzed and the nomenclature used are summarized in Table 2. Four different reinforcement widths b were considered for plates types I and II: 18, 27, 45 and 63 mm. These numbers are used as identifiers in conjunction with the prefixes R (reinforcement—plate type I) and F (frame—plate type II) as shown in the table. These values correspond to a reinforcement width of 10, 15, 25 and 35% of the total plate width, respectively.

Both of these configurations can be easily manufactured and are of practical significance. However, direct comparison of the natural frequencies of various type I and II plates is not meaningful because the structural mass is different for each situation as the volume of reinforcement varies with reinforcement width and the type of reinforcement. Therefore, in order to present a meaningful comparison, the first natural frequencies of plates types I and II are normalized with respect to the first natural frequency of a uniform thickness $[0/90]_s$ plate having the same mass as the reinforced plate under consideration. That is, the lamina thickness of the reference $[0/90]_s$ plate is adjusted such that the masses of the reinforced and reference plates are the same.

A third configuration, plate type III, was designed to take advantage of the fact that $[0/90]_s$ and

Table 1
Material properties used for T300/5208 graphite-epoxy

Property	Value
Longitudinal modulus of elasticity, E_1	154,500 MPa
Transverse modulus of elasticity, E_2	111,30 MPa
In-plane Poisson's ratio, v_{12}	0.304
In-plane shear modulus, G_{12}	6980 MPa
Transverse shear modulus, G_{13}	6980 MPa
Transverse shear modulus, G_{23}	3360 MPa
Longitudinal thermal expansion coefficient, α_1	-0.17e-06°C^{-1}
Transverse thermal expansion coefficient, α_2	23.1e-06°C^{-1}
Ply thickness, t	0.15 mm
Mass density, ρ	1.56 g/cm^3

Table 2
Plate descriptions

Designation	Type	b (mm)
R18	I	18
R27	I	27
R45	I	45
R63	I	63
F18	II	18
F27	II	27
F45	II	45
F63	II	63
M0	III	0
M1	III	45
M2	III	90
M3	III	135
M4	III	180

$[90_4]$ square plates of the same dimensions have equal first natural frequencies. The idea was to form a plate with a central section composed of a $[0/90]_s$ laminate combined with two $[90_4]$ edge strips. The edge strips are parallel to the y-axis and are both of width b, forming a square plate as shown in Fig. 2. Unlike the type I and II plates, the total mass of the type III plates is independent of the width b and equal to the total mass of a homogeneous $[0/90]_s$ laminated plate of the same thickness. Therefore, direct comparisons of natural frequencies for the various cases can be made.

Table 2 summarizes the type III plates analyzed and the nomenclature used to describe them. The two limiting cases are when $b = 0$ (plate M0) and $b = 180$ (plate M4) correspond to con-

ventional $[0/90]_s$ and $[90_4]$ laminated plates, respectively. The type III plates were analyzed for five different cases; that is $b = 0$, 45, 90, 135, 180 mm, respectively (plates M0, M1, M2, M3, M4, respectively). It is noted that the middle three plates M1, M2 and M3 are composed of both laminates $[0/90]_s$ and $[90_4]$. Also, in this sequence of problems the proportion of the $[90_4]$ laminate increases linearly from 0–100% from plate M0–M4. Conversely the proportion of the $[0/90]_s$ laminate decreases linearly from 100–0% in the same sequence.

As an aside, it should be mentioned that although the analyses of the type III plates provides an interesting insight into the problem, these plates are impractical because of the low-strength interface between the three strips of the sub-laminates.

4.2. Numerical results

The plate is discretized into 16 elements arranged in a 4×4 rectangular array. This yields a model with a total of 169 nodes and takes advantage of problem symmetry. Only one fourth of the plate is modelled and three different models are analyzed: one for symmetric modes in both the x- and y-directions; one for a symmetric mode in the x-direction and an anti-symmetric mode in the y-direction; and one for an anti-symmetric mode in the x-direction and a symmetric mode in the y-direction. The possibility of anti-symmetric modes in both the x- and y-directions was not analyzed as this always lead to a higher natural frequency that was not of interest.

The material considered for all analyses is graphite/epoxy T300/5208; the properties are given in Table 1, Adams et al. (1988). The finite element analysis is based on the assumption that the material properties do not vary with temperature. Therefore, a linear thermoelastic problem is solved to compute the thermal residual stress resultants. This approximation is reasonable for most engineering applications and represents an upper bound on reality. A more realistic determination of the residual stresses would account for the variation of the material properties with temperature, Adams et al. (1988) and incorporate a thermochemical model of the cure process, Ciriscioli and Springer (1990) or a model of the consolidation process, Domb and Hansen (1994).

The boundary conditions used for the solution of the thermoelastic problem provide no constraint other than to eliminate rigid-body motion. The solution of the free vibration problem assumes simply supported conditions on all edges of the plate; the application of these boundary conditions imposes no additional residual stresses on the problem.

The natural frequencies and vibration modes of all plates listed in Table 2 were calculated. The idea was to study the influence of the reinforcement type and width as well as the effect of temperature on the natural frequencies. In what follows, the temperature difference, T, is given as a positive number and should be understood to be the difference between an elevated temperature at which the plate and reinforcement are stress free (cure, consolidation, or secondary bonding temperature) and a lower temperature (operating or room temperature) of the structure.

The reinforcement type primarily affects the distribution of thermal residual stress resultants. This is illustrated in Figs 3a and 3b. (Only one fourth the plate is shown because of the symmetry of the problem.) The results compare the distribution of thermal residual stress resultants N_y^R in plates F18 and R18 for a temperature difference of 150°C. It can be seen that in plate R18 the distribution of the stress resultant N_y^R exhibits large gradients near the edge of the reinforcement. It should be noted that plate F18, in which the reinforcement forms a frame around the perimeter of the plate, yields a smoother stress distribution than plate R18. Furthermore, the stress resultant

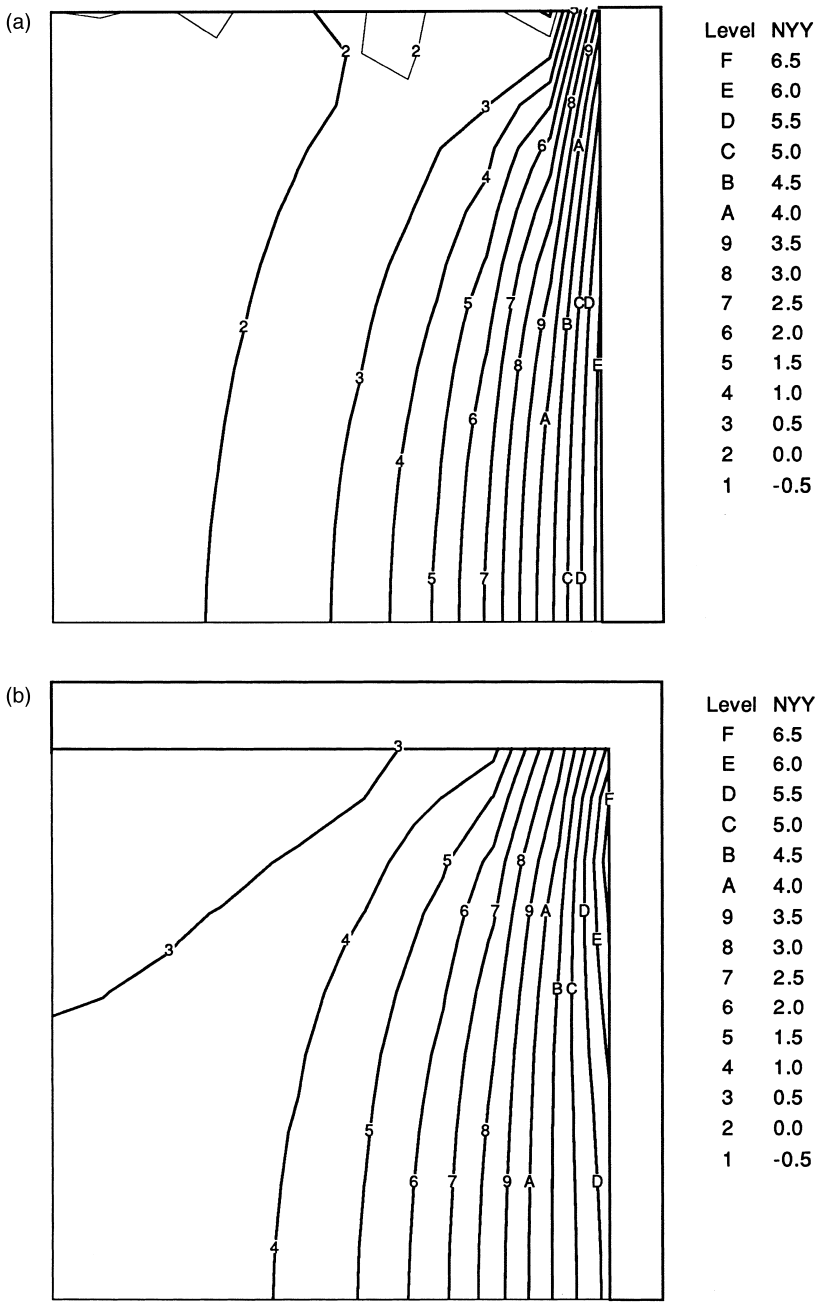

Fig. 3. (a) Distribution of thermal residual stress resultants N_y^R on plate R18 for a temperature difference of 150°C. (b) Distribution of thermal residual stress resultants N_y^R on plate F18 for a temperature difference of 150°C.

N_y^R is positive everywhere which is reminiscent of a pretensioned drum-membrane and which contributes to an increase of the plate natural frequency.

The existence of thermal residual-stresses affects the vibration modes as well as the natural frequencies of the plate. The thermal residual-stresses vary linearly with the temperature difference; however, the thermal residual-stresses affect each vibration mode differently. Therefore, as the temperature difference is changed the vibration mode may also change. As an example, Figs 4a and 4b show the first vibration modes for plate R45 for $T = 0$ and $T = 150^\circ$C, respectively. Again, only one fourth of the plate is shown because of symmetry. It may be noted that although the mode shapes have changed very little, there has been a dramatic change in natural frequency.

The normalized first natural frequencies as a function of the temperature difference for plates with reinforcement type I are presented in Fig. 5. It can be seen that the variation of the normalized first natural frequency with temperature difference is approximately independent of the reinforcement width, b, within the range considered here. The normalized first natural frequencies of the plates increase by approximately 50% as the temperature difference increases from 0–150°.

Figure 6 shows the normalized first natural frequencies for plates with reinforcement type II. It can be seen that the first natural frequencies increase dramatically with temperature difference. Again, the variation of the normalized first natural frequency with temperature difference is approximately independent of the reinforcement width, b, within the present range. The normalized first natural frequency for $T = 150^\circ$C is typically twice the value for $T = 0^\circ$C. Comparing Figs 5 and 6, it may be concluded that with a small temperature difference, plates with reinforcement types I have a slightly higher structural efficiency in terms of first natural frequency than plates with reinforcement type II; however, as the temperature difference increases reinforcement type II becomes more efficient. This result is due to the differences in the thermal residual-stress states.

The effect of the residual stresses on the higher natural frequencies for plates with reinforcement types I and II are shown in Figs 7a–d. Figure 7a presents the variation of the first three natural frequencies of plates R18 and F18 with temperature difference. It can be seen that the change in the higher natural frequencies is not as pronounced as for the first natural frequency. Also, the effect of temperature difference on the natural frequencies is significantly smaller in plate R18 than in plate F18. Clearly, the distribution of thermal residual stresses in plate F18 is more favourable.

In the particular case of plate R18, the first natural frequency increases by 52% as the temperature difference increases from 0–150°C while in comparison, the second and third natural frequencies increase by 18 and 20%, respectively, for the same interval. On the other hand, the first natural frequency of plate F18 increases by 95% as the temperature difference increases from 0–150°C while the second and third natural frequencies increase by 76 and 35%, respectively. Thus it seems the gains in the higher frequencies, while still very significant, are smaller than those for the first natural frequency. Figures 7b–d illustrate a similar set of results for plates R27, R45 and R63, respectively.

The first natural frequencies of plates with type III reinforcement are compared in Fig. 8 for various temperature differences. Since plates M0 and M4 are homogeneous their vibration response shows no dependence on the temperature difference. On the other hand, the thermal residual-stresses present on plates M1, M2 and M3 strongly influence their first natural frequencies. These results show that the thermal residual-stresses have a beneficial effect on the vibrational behaviour of plate M1. On the other hand, the first natural frequency of plate M2 initially increases with the temperature difference and then starts decreasing. Furthermore, the thermal residual stresses also

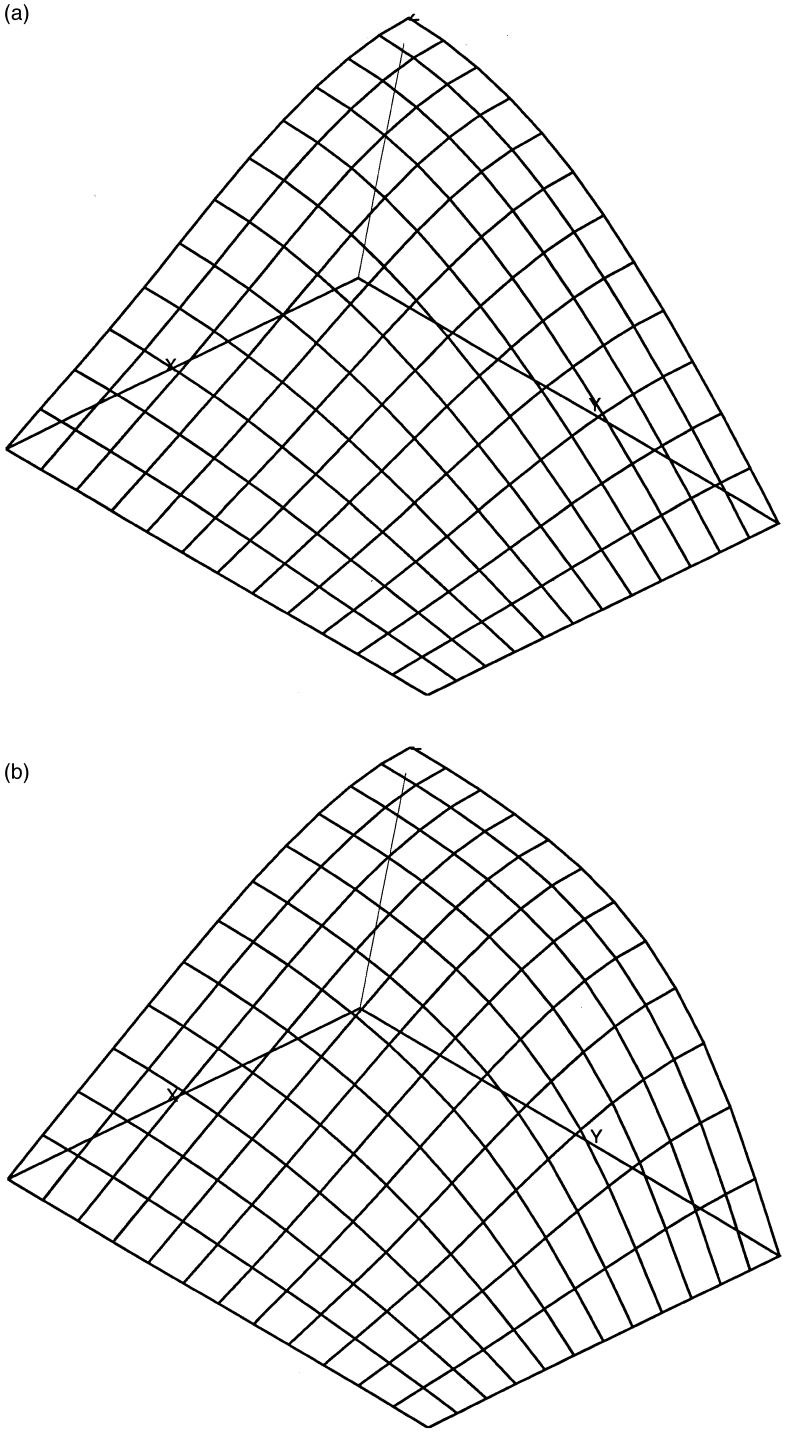

Fig. 4. (a) First vibration mode for plate R45 for a temperature difference of 0°C. (b) First vibration mode for plate R45 for a temperature difference of 150°C.

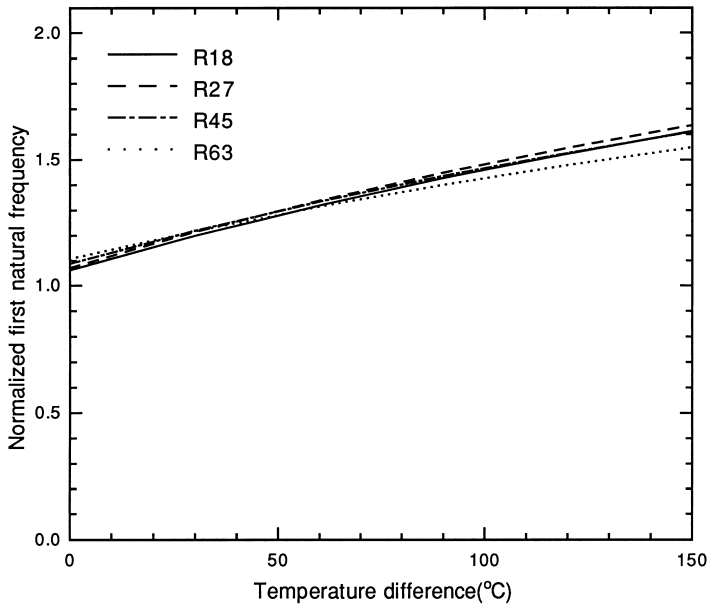

Fig. 5. Normalized first natural frequencies of plates R18, R27, R45 and R63 as a function of the temperature difference T.

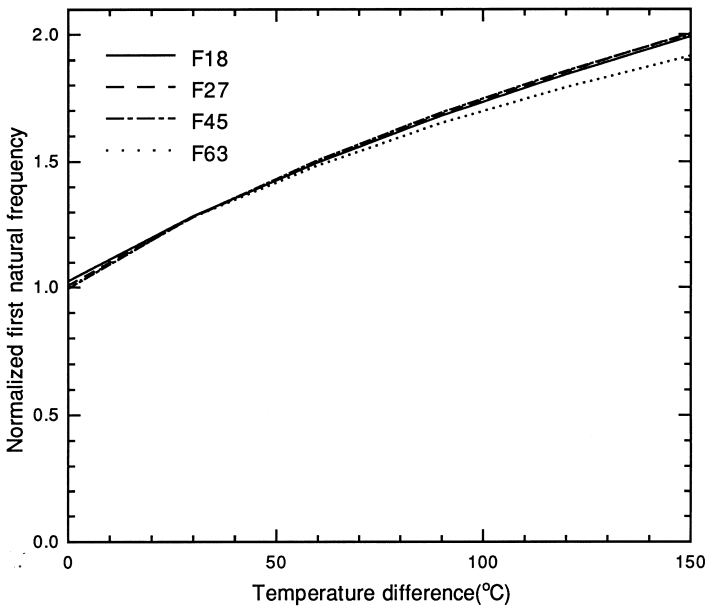

Fig. 6. Normalized first natural frequencies of plates F18, F27, F45 and F63 as a function of the temperature difference T.

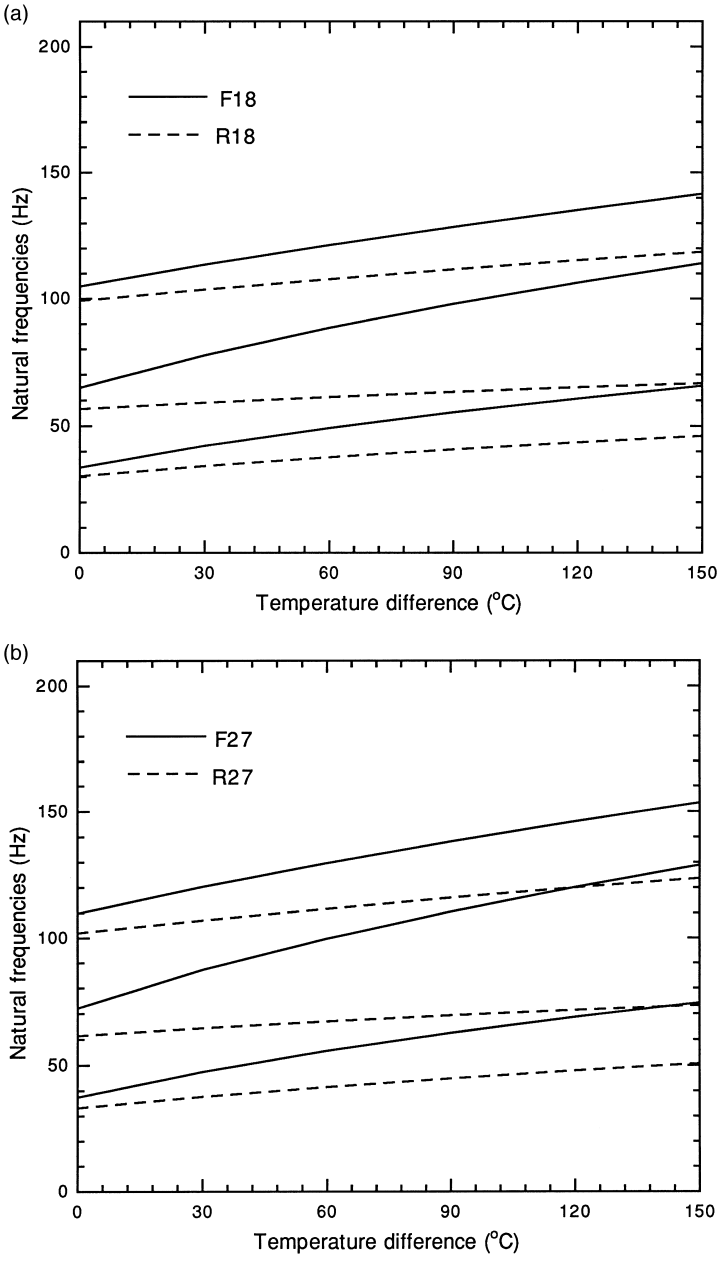

Fig. 7. (a) Natural frequencies of plates R18 and F18 as a function of the temperature difference T. (b) Natural frequencies of plates R27 and F27 as a function of the temperature difference T.

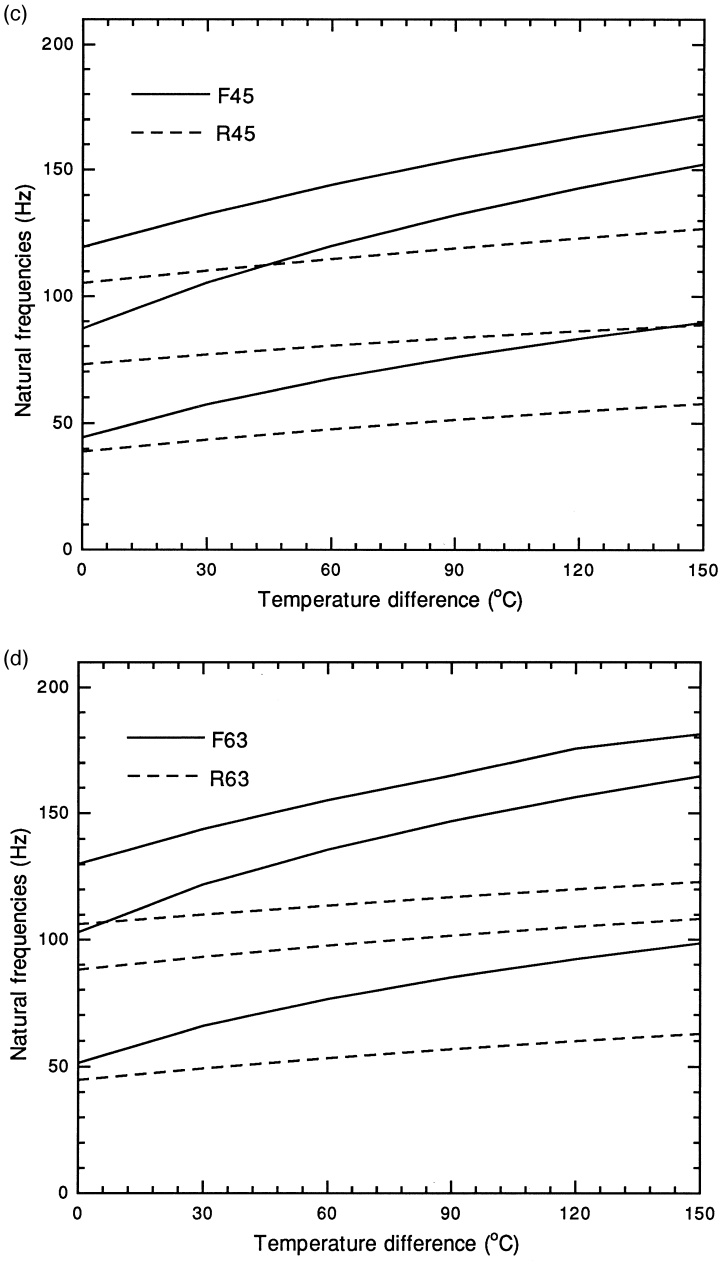

Fig. 7. (c) Natural frequencies of plates R45 and F45 as a function of the temperature difference T. (d) Natural frequencies of plates R63 and F63 as a function of the temperature difference T.

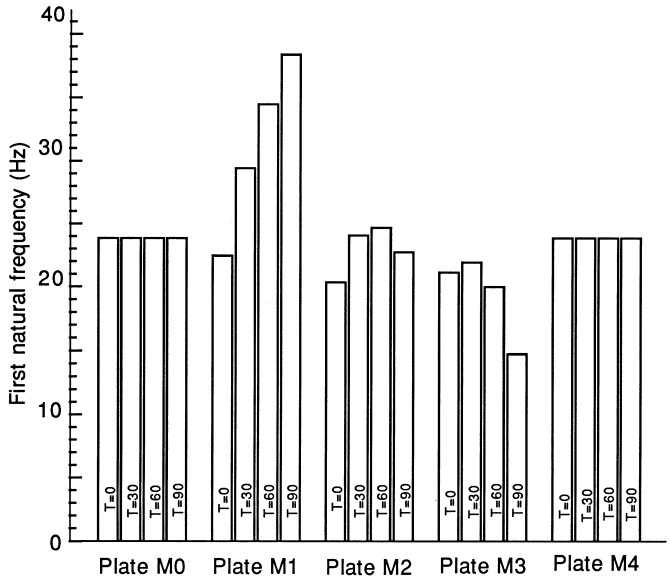

Fig. 8. First natural frequencies of plates M0, M1, M2, M3 and M4 for different values of the temperature difference T.

exhibit a detrimental effect on the first natural frequency of plate M3. In fact, if this plate is processed above a critical temperature, $T \approx 100^{\circ}\mathrm{C}$, it buckles as a result of the thermal stresses and the first natural frequency is zero!

5. Conclusions

The analyses presented here demonstrate that thermal residual-stresses resulting from the elevated temperature manufacture of composite structures may strongly affect natural frequencies. Both the distribution and magnitude of the thermal residual-stresses have been shown to be important. In fact, the first natural frequency can be doubled or reduced to zero as a result of thermoelastic structural effects. Whether these effects are beneficial or detrimental depends on factors such as geometry, boundary conditions, material properties and design. However it is seems clear that, independent of the specific plate geometry, it is possible to use the thermal residual effects to increase natural frequencies.

Based on the results of the present work, it is suggested that, through appropriate design and analysis, thermal residual-stresses may be tailored to enhance a range of the response characteristics of composite structures. As an example, Almeida and Hansen (1996) have demonstrated that thermal residual-stresses may also be used to effectively improve the buckling behaviour of reinforced composite plates. The design process to capitalize on thermoelastic effects involves the choice of the ply orientation, the position and geometry of stringer reinforcement, and the fabrication process. Therefore it also seems that the inclusion of thermoelastic effects within opti-

mization procedures would be very effective for the determination of the design parameters that maximize the composite structural performance.

Finally, it should be emphasized that the simple cases analyzed in this work were specifically chosen to demonstrate the potential increases in natural frequencies. However, actual designs of composite structures require a comprehensive analysis of overall structural behaviour. Tensile thermal residual-stresses may be beneficial for vibration and other elastic behaviour; however, these stresses may have detrimental effects on strength and damage tolerance of composite structures. Therefore, the maximum possible gain in the natural frequency or other structural characteristic may be limited by requirements on overall structural performance. Such a view points even more strongly toward the implementation of the present type of thermoelastic analysis within an optimization capability to truly capitalize on the full range of enhancement possibilities.

Acknowledgements

The first author acknowledges CNPq (Brazilian National Research Council) for the financial support received for this work under Grant 200692/82-8. Additional support came from NSERC (Natural Sciences and Engineering Research Council Canada) Grant OGP0003663.

References

Adams, D.S., Bowles, D.E., Herakovich, C.T., 1988. Thermally induced transverse cracking in graphite-epoxy cross-ply laminates. In: Springer, G.S. (Ed.), Environmental Effects on Composite Materials, Vol. 3. Technomic Publ. Co. Inc., Lancaster, PA, pp. 247–274.

Almeida, S.F.M., Hansen, J.S., 1996. Enhanced elastic buckling loads of composite plates with tailored thermal residual stresses. Technical Report No. 72, Institute of Mechanical Engineering, Aalborg University, Aalborg East, Denmark, October.

Bathe, K.-J., Wilson, E.L., 1976. Numerical Methods in Finite Element Analysis. Prentice-Hall, Englewood Cliffs, NJ.

Brunelle, E.J., Robertson, S.R., 1974. Initially stressed Mindlin plates. AIAA J. 12, 1036–1045.

Ciriscioli, P.R., Springer, G.S., 1990. Smart Autoclave Cure of Composites. Technomic Publ. Co., Inc., Lancaster, PA.

Domb, M.M., Hansen, J.S., 1994. Development of free edge effect during processing of semi-crystalline thermoplastic composites. AIAA J. 31 (5), 1029–1033.

Heppler, G.R., Hansen, J.S., 1986. A Mindlin element for thick and deep shells. Computer Methods in Applied Mechanics and Engineering 54 (1), 21–47.

Herrmann, G., Armenakas, A.E., 1960. Vibrations and stability of plates under initial stress. ASCE Journal of the Engineering Mechanics Division 86, 458–487.

Jones, R.M., 1975. Mechanics of Composite Materials. McGraw-Hill, New York.

Mindlin, R.D., 1951. Influence of rotary inertia and shear on flexural motions of isotropic elastic plates. J. Appl. Mechanics 18, 31–38.

Novozhilov, V.V., 1953. Foundations of the Non-linear Theory of Elasticity. Graylock, Rochester, New York.

Sai Ram, K.S., Sinha, P.K., 1962. Hygrothermal effects on the free vibration of laminated composite plates. Journal of Sound and Vibration 158 (1), 133–148.

Whitney, J.M., Ashton, J.E., 1971. Effect of environment on the elastic response of layered composite plates. AIAA J. 9, 1708–1713.

Yang, I.H., Shieh, J.A., 1987. Vibrations initially stressed thick rectangular orthotropic plates. Journal of Sound and Vibration 119, 545–558.